



A new method for calculating number concentrations of cloud condensation nuclei based on measurements of a three-wavelength humidified nephelometer system

Jiangchuan Tao^{1,2}, Chunsheng Zhao², Ye Kuang^{1,2}, Gang Zhao², Chuanyang Shen², Yingli Yu², Yuxuan Bian³, and Wanyun Xu³

¹Institute for Environment and Climate Research, Jinan University, Guangzhou, China

²Department of Atmospheric and Oceanic Sciences, School of Physics, Peking University, Beijing, China

³State Key Laboratory of Severe Weather, Chinese Academy of Meteorological Sciences, Beijing, China

Correspondence: Chunsheng Zhao (zcs@pku.edu.cn)

Received: 14 June 2017 – Discussion started: 28 July 2017

Revised: 23 December 2017 – Accepted: 2 January 2018 – Published: 14 February 2018

Abstract. The number concentration of cloud condensation nuclei (CCN) plays a fundamental role in cloud physics. Instrumentations of direct measurements of CCN number concentration (N_{CCN}) based on chamber technology are complex and costly; thus a simple way for measuring N_{CCN} is needed. In this study, a new method for N_{CCN} calculation based on measurements of a three-wavelength humidified nephelometer system is proposed. A three-wavelength humidified nephelometer system can measure the aerosol light-scattering coefficient (σ_{sp}) at three wavelengths and the light-scattering enhancement factor (f_{RH}). The Ångström exponent (Å) inferred from σ_{sp} at three wavelengths provides information on mean predominate aerosol size, and hygroscopicity parameter (κ) can be calculated from the combination of f_{RH} and Å . Given this, a lookup table that includes σ_{sp} , κ and Å is established to predict N_{CCN} . Due to the precondition for the application, this new method is not suitable for externally mixed particles, large particles (e.g., dust and sea salt) or fresh aerosol particles. This method is validated with direct measurements of N_{CCN} using a CCN counter on the North China Plain. Results show that relative deviations between calculated N_{CCN} and measured N_{CCN} are within 30 % and confirm the robustness of this method. This method enables simpler N_{CCN} measurements because the humidified nephelometer system is easily operated and stable. Compared with the method using a CCN counter, another advantage of this newly proposed method is that it can obtain N_{CCN} at lower supersaturations in the ambient atmosphere.

1 Introduction

Cloud condensation nuclei (CCN) are the aerosol particles that form cloud droplets by hygroscopic growth. CCN number concentration (N_{CCN}) plays a fundamental role in cloud microphysics and aerosol indirect radiative effect. In general, the direct measurement of N_{CCN} is achieved in a chamber under supersaturated conditions (Hudson, 1989; Nenes et al., 2001; Rose et al., 2008). Due to the requirement of high accuracies of working conditions like temperatures, vapors and flow rates in chambers, the direct measurement of N_{CCN} is complex and costly (Rose et al., 2008; Latham and Nenes, 2011). Thus, developments of simplified measurements of N_{CCN} are required. In recent years, attention has been focused on measurements of aerosol optical properties (Jefferson, 2010; Ervens et al., 2007; Gasso and Hegg, 2003), which are simple and well developed (Covert et al., 1972; Titos et al., 2016). For aerosol population free of sea salt or dust, the accumulation mode aerosol not only dominates aerosol scattering ability but also contributes most to N_{CCN} . Thus, the calculation of N_{CCN} based on measurements of aerosol optical properties is feasible and can facilitate N_{CCN} measurement.

There are methods for calculating N_{CCN} based on measurements of aerosol optical properties. For the first, N_{CCN} as well as the hygroscopicity parameter (κ) can be calculated based on measurements of a humidified nephelometer system in combination with aerosol particle number size distribution (PNSD; Ervens et al., 2007; Chen et al., 2014). Thus addi-

Table 1. Review of studies that have used aerosol optical parameters to infer N_{CCN} .

Campaign	Air mass	Parameter	Caveats	Results	Reference
ICARTT ¹ in the northeastern USA and Canada	Polluted air mass	fRH and PNSD	N_{CCN} calculated with aerosol hygroscopicity constrained by $f(RH)$ and PNSD.	N_{CCN} predicted at SS >0.3 % with a 0.9 R^2 .	Ervens et al. (2007)
HaChi ² on the North China Plain	Aged continental air mass	PNSD and fRH	Similar to Ervens et al. (2007). N_{CCN} calculated with the hygroscopicity parameter constrained by $f(RH)$ and PNSD.	Slopes around 1 and R^2 around 0.9.	Chen et al. (2014)
TARFOX ³ Atlantic seaboard and ACE-2 ⁴	Polluted air mass	Aerosol volume retrieved from remote sensing	N_{CCN} predicted from aerosol volumes with empirical number-to-volume concentration ratio.	Overestimated up to 5 times.	Gasso and Hegg (2003)
ACE-2 in north-eastern Atlantic	Diverse air mass	Backscatter or extinction profile. CCN at the surface.	N_{CCN} profile retrieved from backscatter (or extinction) vertical profile assuming their ratios are the same as the ratio at surface, which can be calculated by backscatter (or extinction) and N_{CCN} measured at the surface.	N_{CCN} predicted on most days for 0.1 % SS and on 20–40 % of the days at 1 % SS.	Ghan and Collins (2004)
ARM ⁵ Climate Research Facility central site at the Southern Great Plains	Continental air mass	Backscatter (or extinction) and RH profile. fRH and CCN at surface	Same as Ghan and Collins (2004).	CCN variance explained for 25–63 % of all measurements at high supersaturations	Ghan et al. (2006)
TRACE-P ⁶ and ACE-Asia ⁷	Asian outflow over the western Pacific	Aerosol index (AI, the product of ambient light extinction and Å)	N_{CCN} predicted based on empirical relationship between AI and N_{CCN} .	AI related well to CCN only with suitably stratified data.	Kapustin et al. (2006)
Multiple measurements	Diverse air mass	AERONET aerosol optical thickness (AOT)	N_{CCN} predicted based on empirical relationship between AOT and N_{CCN} as a power law.	N_{CCN} predicted at SS >0.3 % with a 0.88 R^2 , but with a factor-of-4 range of N_{CCN} at a given AOT.	Andreae (2009)
Four ARM sites	Polluted air mass	SSA, backscatter fraction and σ_{sp}	N_{CCN} estimated from fitting parameters for the N_{CCN} activity spectra, which can be calculated based on their empirical relationships with aerosol optical properties.	N_{CCN} predicted with slopes around 0.9 and R^2 around 0.6.	Jefferson (2010)
Multiple ARM sites around the world	Diverse air mass	RH, fRH , SSA, AOT and σ_{sp}	N_{CCN} calculated with σ_{sp} (or AOT) based on their empirical relationship, which is affected by RH, fRH and SSA.	Best results achieved by using σ_{sp} and SSA. Weak effect on the σ_{sp} – N_{CCN} relationship by fRH . N_{CCN} –AOT relationship deteriorated with increasing RH	Liu and Li (2014)
Multiple ARM sites around the world	Diverse air mass not dominated by dust	Å and extinction coefficient	N_{CCN} calculated with light extinction based on their empirical relationship.	Deviated typically within a factor of 2.0.	Shinozuka et al. (2015)

¹ International Consortium for Atmospheric Research on Transport and Transformation. ² Haze in China. ³ Troposphere Aerosol Radiative Forcing Experiment. ⁴ Second Aerosol Characterization Experiment. ⁵ Atmospheric Radiation Measurement. ⁶ Transport and Chemical Evolution over the Pacific. ⁷ Aerosol Characterization Experiment–Asia.

tional measurements of PNSD are needed. For the second, N_{CCN} is calculated based on statistical relationships between N_{CCN} and aerosol optical properties, such as scattering coefficient (σ_{sp}), Ångström exponent (Å) and single-scattering albedo (SSA; Jefferson, 2010; Shinozuka et al., 2015). Å is

the exponent commonly used to describe the dependence of σ_{sp} on wavelength as the formula shows:

$$\sigma_{sp}(\lambda) = \beta \cdot \lambda^{-\text{Å}}, \quad (1)$$

where β is the aerosol number concentration. The coefficient of determination (R^2) between measured and calculated N_{CCN} using the first method is about 0.9. For the second method, R^2 is generally lower than 0.9, although the instruments are cheaper and easier in operation. Applications similar to the second method are widely used in remote sensing. As shown in Table 1, earlier studies found that the aerosol volume or aerosol PNSD retrieved from remote sensing measurements can be used to calculate N_{CCN} (Gasso and Hegg, 2003; Kapustin et al., 2006). Recently, either aerosol optical depth (AOD) or aerosol vertical profile has been used to predict N_{CCN} directly (Ghan and Collins, 2004; Ghan et al., 2006; Andreae, 2009; Liu and Li, 2014).

In the statistical relationship between N_{CCN} and aerosol optical properties, σ_{sp} or AOD is mainly the proxy of aerosol absolute concentration, while \dot{A} or SSA can be used to reveal the variations of aerosol CCN activity, as shown in Table 1. Based on Köhler theory (Köhler, 1936; Petters and Kreidenweis, 2007), aerosol CCN activity is determined by aerosol size and aerosol chemical composition, and aerosol chemical composition can be defined as aerosol hygroscopicity. Information about aerosol size and aerosol hygroscopicity is critical to N_{CCN} prediction, and their absence can lead to a deviation by a factor of 4 (Andreae, 2009). Compared with aerosol hygroscopicity, aerosol size is more important in determining CCN activity (Dusek et al., 2006). The value of \dot{A} can provide information on mean predominate aerosol size (Brock et al., 2016; Kuang et al., 2017a). As a result, N_{CCN} calculation from \dot{A} and the extinction coefficient is found to be accurate to some extent (Shinozuka et al., 2015). As proxies for aerosol hygroscopicity, SSA or aerosol light-scattering enhancement factor (fRH) is commonly used, albeit not so effective (Jefferson, 2010; Liu and Li, 2014). fRH is defined as

$$fRH = \sigma_{sp}(RH) / \sigma_{sp}, \quad (2)$$

where $\sigma_{sp}(RH)$ is the humidified σ_{sp} at a given relative humidity (RH). SSA is determined by the ratio between the light-absorbing carbonaceous and less-absorbing components. Black carbon dominates the absorption of solar radiation and is a main hydrophobic component as well. Less-absorbing components consist of inorganic salts and acids, as well as most organic compounds, which are generally hygroscopic components. SSA correlates positively with aerosol hygroscopicity (Rose et al., 2010) but deviates significantly due to the diversity of hygroscopicity of less-absorbing components. Thus N_{CCN} calculation combining SSA, backscatter fraction and σ_{sp} still leads to significant deviations, with $R^2 = 0.6$ (Jefferson, 2010). As for fRH , there was a study that applied aerosol optical quantities (σ_{sp} or aerosol optical thickness) with fRH or SSA to calculate N_{CCN} (Liu and Li, 2014). In their study, compared with the combination of SSA and aerosol optical quantities, the combination of fRH and aerosol optical quantities is found to be less accurate in estimating N_{CCN} , even though fRH is directly connected

with aerosol hygroscopicity (Liu and Li, 2014). This may result from the significant dependence of fRH on aerosol size (Chen et al., 2014; Kreidenweis and Asa-Awuku, 2014; Kuang et al., 2017a). As mentioned before, PNSD is needed for better calculation of κ and N_{CCN} from fRH in previous studies (Ervens et al., 2007; Chen et al., 2014). A new method to estimate κ from fRH and \dot{A} was proposed recently (Kuang et al., 2017a; Brock et al., 2016). Based on this method, fRH can be used to calculate N_{CCN} without measurements of PNSD and can be expected to improve the N_{CCN} prediction just based on measurements of aerosol optical properties.

In this study, the relationship between N_{CCN} and aerosol optical properties measured by a humidified nephelometer system is studied and a new method for N_{CCN} prediction is proposed. This new method is validated based on data observed in the Gucheng campaign on the North China Plain and can be expected to improve measurements of N_{CCN} due to advantages of applying nephelometers.

2 Methodology

2.1 Data

Data in this study are mainly measured at Gucheng (39.15° N, 115.74° E) during autumn in 2016 on the North China Plain. Gucheng is 100 km southwest from Beijing and 40 km northeast from Baoding and has background pollution conditions on the North China Plain. The observation site was surrounded by farmland and about 3 km away from the town of Gucheng. This campaign started on 20 October and lasted for nearly 1 month.

Instruments used in the Gucheng campaign were located in a measurement container under temperature maintained at 25 °C. Ambient aerosol was sampled and dried to RH lower than 30 % by an inlet system consisting of a PM10 inlet, in-line Nafion dryers, and a RH and temperature sensor (Vaisala HMP110). Then the sample aerosol was separated by a splitter and directed into various instruments. During this campaign, σ_{sp} , fRH , particle-size-resolved activation ratio (AR) and PNSD were obtained.

fRH and σ_{sp} at three wavelengths were measured by a humidified nephelometer system consisting of two nephelometers (Aurora 3000, Ecotech Inc.) and a humidifier. In addition, \dot{A} can be calculated directly from σ_{sp} measured by a nephelometer. The humidifier with a Gore-Tex tube humidified the sample air up to 90 % RH. A whole cycle of humidification from 50 to 90 % RH lasted about 45 min. Dried σ_{sp} was obtained directly from dried sample aerosol measured by one nephelometer, and humidified σ_{sp} was obtained from humidified aerosol measured by another nephelometer. fRH can be calculated by dividing humidified σ_{sp} by dried σ_{sp} . Detailed description of the humidified nephelometer system was illustrated in Kuang et al. (2017a).

The particle-size-resolved AR, defined as the ratio of N_{CCN} to total particles at a specific particle size, was measured by a system mainly consisting of a differential mobility analyzer (DMA, model 3081) and a continuous-flow CCN counter (model CCN200, Droplet Measurement Technologies, USA; Roberts and Nenes, 2005; Lance et al., 2006). The system selected mono-disperse particles with the DMA coupled with an electrostatic classifier (model 3080; TSI, Inc., Shoreview, MN USA) and measured AR of the mono-disperse particles by a condensation particle counter (CPC model 3776; TSI, Inc.) and CCN counter. Ranges of particle size and supersaturation (SS) were 10–300 nm and 0.07–0.80 %, respectively. Measurements at five supersaturations (0.07, 0.10, 0.20, 0.40 and 0.80 %) were conducted sequentially with each cycle lasting for 1 h, and N_{CCN} at 0.07 % supersaturation was used in this study. Due to non-idealities of the CCN counter at supersaturations lower than 0.10 %, CCN measurement at 0.07 % supersaturation was found to be the most uncertain (Rose et al., 2008) and can lead to deviations of measured N_{CCN} in this study. Before and after the campaign, supersaturations set in this system were calibrated using ammonium sulfate (Rose et al., 2008). More information about the system is available in Deng et al. (2011) and Ma et al. (2016).

PNSD with a particle diameter from 9 nm to 10 μm was measured by a mobility particle size spectrometer (SMPS, TSI Inc., model 3996) and an aerodynamic particle sizer (APS, TSI Inc., model 3321). SMPS consisted of a DMA, an electrostatic classifier and a CPC (model 3776; TSI, Inc., Shoreview, MN USA) and measured PNSD with a diameter lower than 700 nm.

In addition, PNSD and σ_{sp} from 2011 to 2014 during four campaigns (Wuqing in 2011, Xianghe in 2012 and 2013, and Wangdu in 2014) in the North China Plain were used in this study. PNSD in these campaigns was measured by a twin differential mobility particle sizer (TDMPS, Leibniz Institute for Tropospheric Research (IfT), Germany) and an APS (TSI Inc., model 3321). A TSI 3563 nephelometer was used to obtain σ_{sp} at three wavelengths. Details about the four campaigns can be found in Ma et al. (2011, 2016) and Kuang et al. (2016, 2017a).

2.2 Theories

Hygroscopic growth of particles at a certain relative humidity can be described by κ -Köhler theory (Petters and Kreidenweis, 2007):

$$\frac{RH}{100} = \frac{g(RH)^3 - 1}{g(RH)^3 - (1 - \kappa)} \cdot \exp\left(\frac{4\sigma_{s/a} \cdot M_w}{R \cdot T \cdot D_d \cdot g(RH) \cdot \rho_w}\right), \quad (3)$$

where $g(RH)$ is the geometric diameter growth factor; κ is the hygroscopicity parameter; RH is the relative humidity; ρ_w is the density of water; M_w is the molecular weight of water; $\sigma_{s/a}$ is the surface tension of the solution–air interface, which is assumed to be equal to the surface tension of the

pure water–air interface; R is the universal gas constant; and T is the temperature.

When accounting for the impact of \dot{A} , κ_f can be derived directly from fRH (Brock et al., 2016; Kuang et al., 2017a). A single-parameter parameterization scheme proposed by Brock et al. (2016) connects fRH and κ by the approximately proportional relationship between total aerosol volume and σ_{sp} :

$$f(RH) = 1 + \kappa_{sca} \times RH / (100 - RH), \quad (4)$$

where κ_{sca} is a parameter for fitting fRH curves and can be used to predict κ_f in combination with \dot{A} as in recent studies (Brock et al., 2016; Kuang et al., 2017a). This method of calculating κ_f based on κ_{sca} and \dot{A} was confirmed by good agreement with κ_f calculated from fRH and PNSD.

N_{CCN} can be calculated from size-resolved AR at a certain SS and PNSD (referred to as $n(\log D_p)$) as follows:

$$N_{CCN} = \int_{\log D_p} AR(\log D_p, SS) \cdot n(\log D_p) d \log D_p. \quad (5)$$

In general, size-resolved AR curves are complicated and always replaced by a critical diameter (D_c) to simplify calculation (Deng et al., 2013). The critical diameter is defined as

$$N_{CCN} = \int_{\log D_c}^{\log D_{p,max}} n(\log D_p) d \log D_p, \quad (6)$$

where $D_{p,max}$ is the maximum diameter of the measured PNSD. In other words, the integral of PNSD larger than D_c equals the measured N_{CCN} . And a critical κ (κ_c) can be calculated by Eq. (3) and indicates CCN activity and hygroscopicity of particles.

3 Results

3.1 Calculation of N_{CCN} based on measurements of a humidified nephelometer system

Free of sea salt aerosol and dust aerosol, accumulation mode aerosol dominates both the optical scattering ability at short wavelengths and the CCN activity at low supersaturations, and thus a reasonable relationship between σ_{sp} and N_{CCN} can be achieved. Figure 1 shows the size distribution of cumulative contributions of σ_{sp} at 450 nm and N_{CCN} at 0.07 % with various \dot{A} and κ_c , and corresponding normalized PNSDs based on data measured during the four campaigns on the North China Plain. During the four campaigns, no sea salt aerosol or dust aerosol was observed (Ma et al., 2011, 2016; Kuang et al., 2016, 2017a). For continental aerosol without sea salt or dust, \dot{A} varies from 0.5 to 1.8, and κ_c varies from 0.1 to 0.5 (Cheng et al., 2008; Ma et al., 2011; Liu et al., 2014; Kuang et al., 2017b). As mentioned before, \dot{A} can be

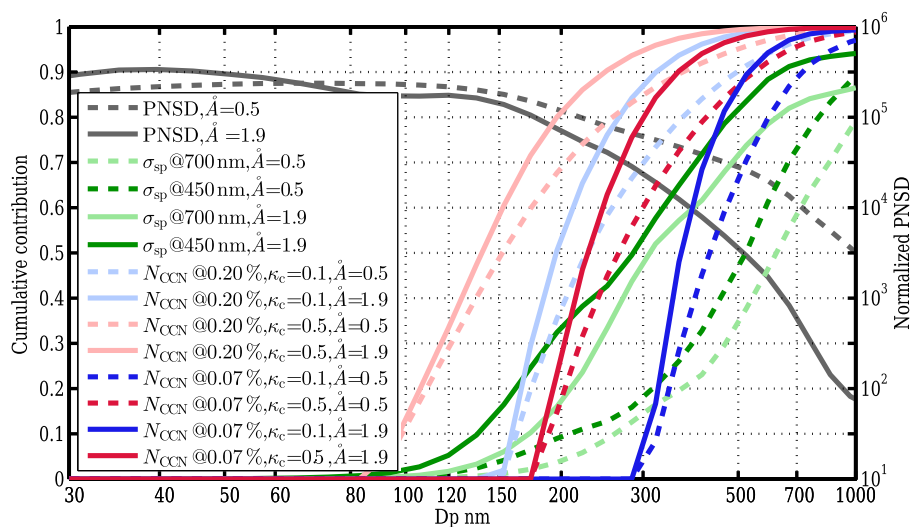


Figure 1. Aerosol PNSD (black lines), the cumulative contribution of σ_{sp} at wavelength of 450 and 700 nm (dark green lines and light green lines, respectively), the cumulative contribution of N_{CCN} at a supersaturation of 0.07 % (dark red and dark blue lines) and the cumulative contribution of N_{CCN} at a supersaturation of 0.20 % (light red and light blue lines) based on measurement in several campaigns in the North China Plain. Solid lines and dashed lines indicate \dot{A} of 1.9 and 0.5, respectively. Blue lines and red lines indicate κ_c of 0.1 and 0.5, respectively.

used as a proxy of the overall size distribution of aerosol populations, with smaller \dot{A} indicating more larger particles. In Fig. 1, comparisons for \dot{A} are made between 0.5 and 1.9 and for κ_c are made between 0.1 and 0.5. As larger particles contribute more to light scattering and CCN activation, cumulative contributions of both σ_{sp} and N_{CCN} increase significantly at the diameter range of accumulation mode particles. Because more hygroscopic particles are able to activate at smaller diameters, the cumulative contribution of N_{CCN} with higher κ_c increases at smaller diameters. In general, major contributions of both σ_{sp} and N_{CCN} are made by particles from 200 to 500 nm for various \dot{A} and κ_c . This implies the feasibility of inferring N_{CCN} from aerosol optical properties.

Because particles smaller than 200 nm can activate at supersaturations higher than 0.07 % while scattering less light at wavelengths longer than 450 nm, which are shown as the light-color lines in Fig. 1, it is obvious that significant differences will exist between cumulative contributions of σ_{sp} and N_{CCN} . This means σ_{sp} and N_{CCN} are dominated by different particles, and poor correlation between σ_{sp} and N_{CCN} can be expected. Thus the method of inferring N_{CCN} from aerosol optical properties is applicable for shorter wavelengths and lower supersaturations.

Furthermore, PNSD with higher \dot{A} indicates more Aitken mode particles and fewer accumulation mode particles. Thus large particles contribute less for both σ_{sp} and N_{CCN} when \dot{A} are higher, characterizing an increase of cumulative contribution curves at smaller diameters. In detail, cumulative contribution curves of σ_{sp} at 1.9 \dot{A} are about 0.3 higher than these curves at 0.5 \dot{A} in the size range of 200 to 700 nm, while cumulative contribution curves of N_{CCN} at 1.9 \dot{A} are 0.2 no

higher than these curves at 0.5 \dot{A} . Changes of cumulative contributions of N_{CCN} and σ_{sp} with various \dot{A} reveal that the shape of PNSD can influence the correlation between N_{CCN} and σ_{sp} . This is confirmed by previous studies in which \dot{A} is found to play an important role in calculating N_{CCN} from σ_{sp} (Shinozuka et al., 2015; Liu and Li, 2014).

The relationship between σ_{sp} and N_{CCN} dependent on \dot{A} and κ_c is evaluated by calculating σ_{sp} and N_{CCN} with different PNSDs (classified by \dot{A}) and different κ_c . In detail, ratios of N_{CCN} to σ_{sp} , referred to as AR_{sp} , are calculated to eliminate the effect of variations of particle concentrations consistent at all diameters. Results at a supersaturation of 0.07 % are shown in Fig. 2, and AR_{sp} is higher than 0 and lower than 10. In general, AR_{sp} are higher for more hygroscopic particles or smaller particles. As particles become more hygroscopic, more CCN can be expected when σ_{sp} is fixed. As aerosol populations consist of more smaller CCN-active particles, the increase of σ_{sp} is weaker than that of N_{CCN} . For example, particles with diameters slightly larger than D_c contribute less to σ_{sp} than particles with diameters much larger than D_c .

In detail, the sensitivity of AR_{sp} to \dot{A} also changes with \dot{A} and κ_c . When \dot{A} are higher than 1.4 and κ_c is lower than 0.2, AR_{sp} is insensitive to \dot{A} ; while when \dot{A} are lower than 1 and κ_c are higher than about 0.3, AR_{sp} is more sensitive to \dot{A} than κ_c . This higher sensitivity of AR_{sp} to \dot{A} reveals that, if the mean predominate size of particles is smaller, the increase of N_{CCN} due to the increase of \dot{A} mentioned in the previous paragraph can be larger as a result. This is the consequence of the sensitivity of AR_{sp} to \dot{A} resulting from the variation of small CCN-active particles, as mentioned before.

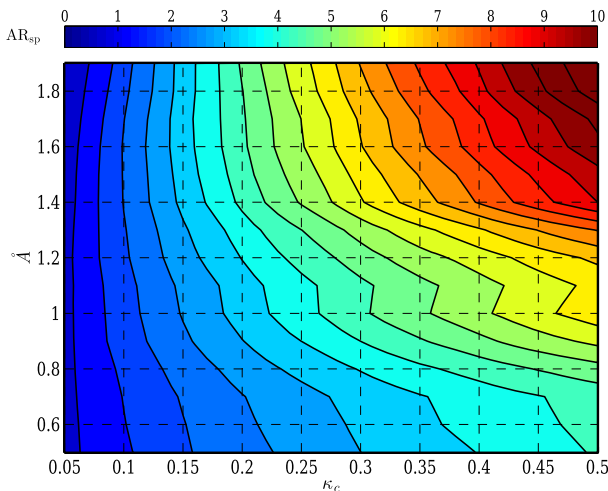


Figure 2. Colors represent AR_{sp} (calculated as $AR_{sp} = \frac{N_{CCN}}{\sigma_{sp}}$ at 450 nm wavelength and 0.07 % supersaturation) with different PNSDs (classified by \dot{A} values) and different κ_c .

Based on the lookup table illustrated in Fig. 2, N_{CCN} at a supersaturation of 0.07 % can be calculated simply from \dot{A} , κ_f and σ_{sp} , which can be obtained from measurements of a three-wavelength humidified nephelometer system. The description of this simple method is shown in Fig. 3. A new lookup table needs to be made for N_{CCN} estimation at other supersaturations, which should ideally be less than 0.07 % as mentioned in the caption of Fig. 1.

One critical issue about the method is the conversion of the κ_f obtained from the humidified nephelometer system to the κ_c under supersaturated conditions. There are two main factors making this conversion necessary. First, closure studies of aerosol hygroscopicity found significant deviations between hygroscopicity at sub-saturated conditions and supersaturated conditions (Wex et al., 2009; Irwin et al., 2010; Good et al., 2010; Renbaum-Wolff et al., 2016). Their difference can be expected to be about 0.1 for accumulation mode aerosol (Wu et al., 2013; Whitehead et al., 2014; Ma et al., 2016). Second, κ_f indicates the hygroscopicity of total particles and can be quite different from aerosol hygroscopicity at a specific diameter due to variations of size-dependent particle hygroscopicity. Kuang et al. (2017a) found a difference around 0.1 between κ_f and κ_c inferred from $g(RH)$ measurements for accumulation mode particles whose κ_f is no larger than 0.2. In this study, a simple conversion wherein κ_c is 0.2 higher than κ_f is used to calculate N_{CCN} , while for κ_f larger than 0.2, a smaller difference of 0.1 between κ_c and κ_f should be used (Kuang et al., 2017a). This simplified relationship between κ_c and κ_f is a rough estimate regardless of the complexity of differences of aerosol hygroscopicity measured by different instruments, but it is still used in this study for two reasons. First, the accurate conversion cannot be achieved without detailed information of the particle hygroscopicity, which is difficult and complicated to measure.

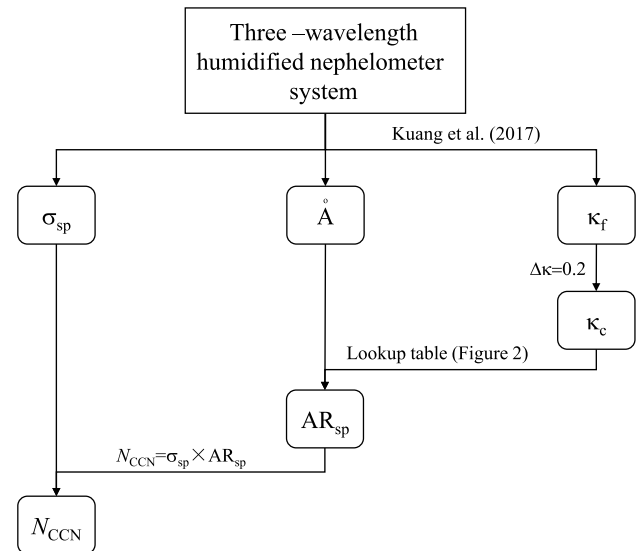


Figure 3. The schematic chart of the N_{CCN} prediction based on measurements of a humidified nephelometer system.

Second, a deviation of κ_c less than 0.1 generally leads to a deviation of N_{CCN} less than 20 % (Ma et al., 2016), which is comparable with the deviation of CCN measurements. As a result, for a simple method of N_{CCN} calculation, this simple conversion is applicable. In addition, it is important to note that the value of the difference between κ_c and κ_f is also a rough estimate regardless of the complexity of aerosol hygroscopicity under different conditions, and the influence of $\Delta\kappa$ deviation on N_{CCN} calculation needs to be further examined based on field observation. For fresh aerosol, the actual $\Delta\kappa$ can be too large (about 4 times the κ values for some organic components; Wex et al., 2009; Renbaum-Wolff et al., 2016) or too small (nearly zero for inorganic components and black carbon) and thus is not suitable for the application of this method.

Besides aerosol size and hygroscopicity, the aerosol mixing state can also affect aerosol CCN activity. When primary aerosol emissions are strong, aerosol populations are likely to be externally mixed and a realistic treatment of aerosol mixing state is critical for N_{CCN} calculation (Cubison et al., 2008; Wex et al., 2010). But for regions away from strong aerosol primary emissions, the influence of mixing state on aerosol CCN activity is small and the assumption of internal mixing state is effective for the estimation of N_{CCN} (Dusek et al., 2006; Deng et al., 2013; Ervens et al., 2010). For regions above the boundary layer where clouds form and measurements of N_{CCN} are important, aerosol generally tends to be internally mixed when there is no strong vertical transport (McMeeking et al., 2011; Ferrero et al., 2014) and there are no plumes (Moteki and Kondo, 2007; McMeeking et al., 2011). In addition, it should be noted that influences of aerosol hygroscopicity and aerosol size on aerosol CCN ac-

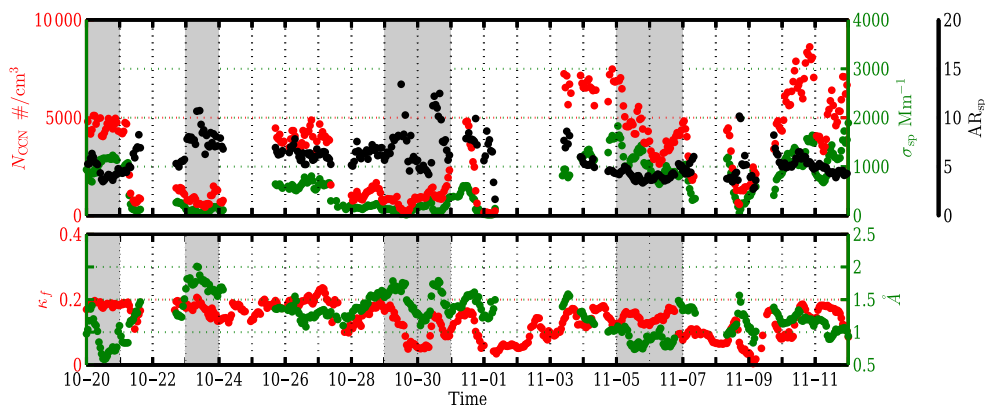


Figure 4. Overview of measurements in Gucheng in 2016. Upper plot: time series of N_{CCN} at a supersaturation of 0.07 % (red dots); σ_{sp} at the wavelength of 50 nm (green dots); and their ratios (black dots), referred to as AR_{sp} . Lower plot: time series of κ_f (red dots) and \bar{A} (green dots). The grey bars are periods when the sensitivity of AR_{sp} to κ_c is notable.

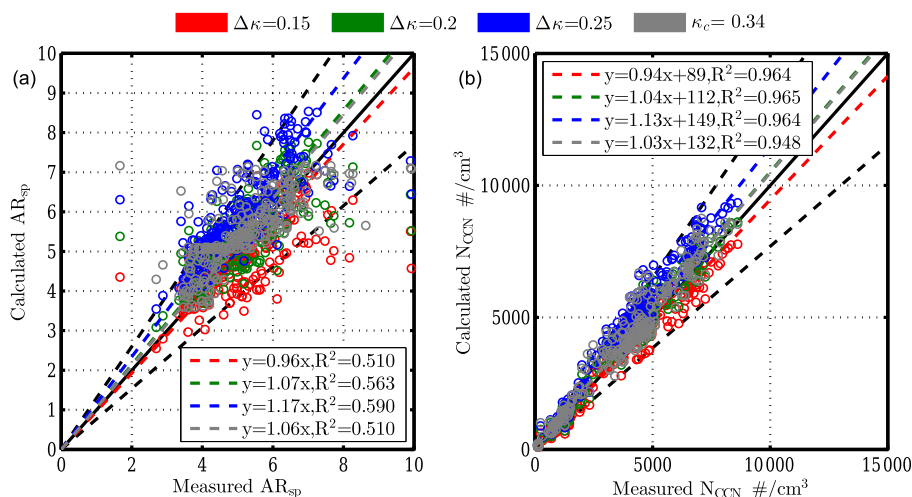


Figure 5. (a) Comparisons of calculated AR_{sp} and measured AR_{sp} with different conversions of κ_c from κ_f . (b) Regressions of calculated N_{CCN} and measured N_{CCN} with different conversions of κ_c from κ_f .

tivity are more significant than the aerosol mixing state and the deviation of N_{CCN} calculation due to the assumption that the aerosol mixing state is smaller than the deviation due to aerosol size and aerosol hygroscopicity. In the new method of this paper, using \bar{A} and κ_c to indicate the influence of aerosol size and aerosol hygroscopicity on aerosol CCN activity will increase the deviation of N_{CCN} calculation, which is much larger than the deviation due to the assumption of aerosol mixing state. As a result, the improvement of N_{CCN} calculation by introducing a more detailed mixing state than internal mixing is limited, and aerosol populations are assumed to be internally mixed for simplification. Thus this method might not be applicable for regions or air masses greatly affected by strong primary aerosol emissions. Furthermore, this new method cannot be applied for regions where sea salt or dust prevails, as mentioned before. In summary, this method can be used to calculate N_{CCN} for air mass tending to be domi-

nated by aged aerosol particles, like continental regions and cloud-forming heights.

3.2 Validation based on N_{CCN} measurement

The method for calculating N_{CCN} based on measurements of the humidified nephelometer system, including the conversion of κ_c and the lookup table, is examined using data measured in Gucheng.

An overview of the data from Gucheng is shown in Fig. 4. From polluted periods to clean periods, significant variations of N_{CCN} and σ_{sp} can be found, but AR_{sp} of N_{CCN} to σ_{sp} stays around 5. On 23 and 29 October, N_{CCN} and σ_{sp} are lower than 2000 # cm^{-3} and 500 Mm^{-1} , respectively; while on 20, 26 October and 3 November, N_{CCN} and σ_{sp} are higher than 2000 # cm^{-3} and 500 Mm^{-1} , respectively. These variations of N_{CCN} and σ_{sp} are mainly due to the variation of the

particle number concentration rather than the shape of particle size distribution and aerosol hygroscopicity. Variations of AR_{sp} result from the variations of \dot{A} and κ_c , which indicate the variations of aerosol microphysical properties and chemical compositions.

In general, AR_{sp} is more sensitive to variations of \dot{A} than κ_c . As mentioned before, the sensitivity of AR_{sp} to \dot{A} is determined by both \dot{A} and κ_f . In detail, \dot{A} during the campaign mainly ranges from 0.5 to 1.5, and κ_f ranges mainly from 0.05 to 0.2, which means that κ_c ranges from 0.25 to 0.4. These values of \dot{A} and κ_f correspond to a significant sensitivity of AR_{sp} to \dot{A} , as the lookup table shows in Fig. 2. The sensitivity of AR_{sp} to κ_c is much smaller and only notable during some short periods (grey bars in Fig. 4). For example, from 5 to 7 November, variations of κ_f and \dot{A} are opposite and result in nearly constant AR_{sp} ; from 30 October to 2 November, consistent variations of \dot{A} and κ_f lead to greater variations of AR_{sp} than other periods. This weak sensitivity of AR_{sp} to κ_f may be due to the uncertainty of κ_c calculated from κ_f based on the simplified conversion.

Based on the lookup table of κ_c and \dot{A} , AR_{sp} is calculated and applied to calculate N_{CCN} with σ_{sp} . The calculated AR_{sp} and N_{CCN} are compared with the measured AR_{sp} and N_{CCN} , shown as the green dots in Fig. 5. In general, good agreements between calculations and measurements are achieved, and relative deviations are within 30%. For the comparison of AR_{sp} , the system relative deviation is less than 10%. For the comparison of N_{CCN} , the slope and the correlation coefficient of the regression are 1.03 and 0.966, respectively.

In addition, the variation of $\Delta\kappa$ and its influence on AR_{sp} and N_{CCN} calculation are studied. As shown in Fig. 6, $\Delta\kappa$ is around 0.2 and independent from \dot{A} and κ_c , and over 80% of $\Delta\kappa$ ranges from 0.1 to 0.3. A notable deviation of $\Delta\kappa$ can only be found when \dot{A} is higher than 1.5. High values of \dot{A} represent existences of small particles, which tend to be freshly emitted and experience inefficient aging processes. In this case, this simplified conversion of κ_c may not be applicable. Furthermore, $\Delta\kappa$ with different values are applied in the new method to calculate N_{CCN} . In the first way, $\Delta\kappa$ of the κ_c conversion is set to be 0.05 higher or lower than 0.2, which means $\Delta\kappa$ of 0.25 or 0.15. The corresponding results are presented as the red dots and blue dots in Fig. 5. In the second way, a constant κ_c of 0.34, which is the average of the κ_c values in the Gucheng campaign, is used to calculate AR_{sp} and N_{CCN} ; it is shown as the grey dots in Fig. 5. In general, differences among calculations using various κ_c conversions are quite small. The $\Delta\kappa$ difference of 0.05 in κ_c conversion only leads to a difference of 10% for the system relative deviation of calculated N_{CCN} . The correlation coefficient of the calculation using a constant κ_c is just a little lower than correlation coefficients of calculations using a κ_c conversion. As a result, for data measured in the Gucheng campaign, the method of calculating N_{CCN} is insensitive to the uncertainty of the κ_c conversion, and a $\Delta\kappa$ of 0.2 is applicable in this new method.

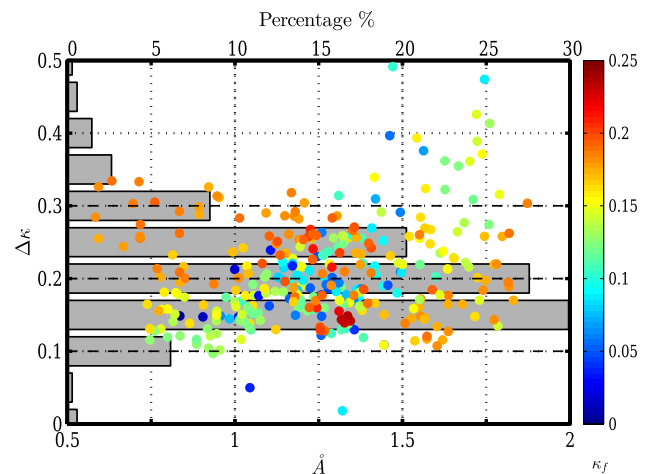


Figure 6. Differences between κ_c and κ_f , referred to as $\Delta\kappa$, with \dot{A} (positions of dots) and κ_f (colors of dots). Bars represent percentages of $\Delta\kappa$ within different ranges.

In this study, the insensitivity of calculated N_{CCN} -to- κ_c conversion is partly due to the small variation of κ_f during the campaign. However, the variation of κ_c can be quite large and cause unignorable deviations of calculated N_{CCN} . As previous studies of N_{CCN} measurement have shown, the variation of κ_c is often small, and a constant κ_c can be used to calculate N_{CCN} accurately (Andreae and Rosenfeld, 2008; Gunthe et al., 2009; Rose et al., 2010; Deng et al., 2013). Results in this study are similar to these previous studies. But large variations of κ_c are also found in some other studies. In the North China Plain, fluctuations of aerosol hygroscopicity during new-particle-formation events and soot emissions lead to significant deviations of calculated N_{CCN} from average aerosol hygroscopicity (Ma et al., 2016). Furthermore, the influence of κ_c cannot be ignored because the value of the average hygroscopicity is different in various regions during various periods. In summer of the North China Plain, measured κ_f at sub-saturated conditions can reach up to 0.45 when inorganic components dominate in particles (Kuang et al., 2016). In this case, calculated N_{CCN} ignoring κ_c may be 10 times larger than measured N_{CCN} . To sum up, although the exact value of κ_c cannot be obtained from the measurement of the humidified nephelometer system, the influence of κ_c on N_{CCN} can be inferred and is found to be correct enough considering the convenience of this method. More data, especially from observations of more hygroscopic aerosol, are still needed to confirm this method.

4 Conclusions

N_{CCN} is a key parameter of cloud microphysics and aerosol indirect radiative effect. Direct measurements of N_{CCN} are generally conducted under supersaturated conditions in CCN chambers, and are complex and costly. Accumulation mode aerosol contributes most to both the aerosol scattering ability and the aerosol CCN activity. In view of this, it is possible to predict N_{CCN} based on relationships between aerosol optical properties and the aerosol CCN activity. In this study, a new method is proposed to calculate N_{CCN} based on measurements of a humidified nephelometer system. In this method, N_{CCN} is derived from a lookup table which involves σ_{sp} , \AA and κ_f , and the required three parameters can be obtained from a three-wavelength humidified nephelometer system.

Relationships between aerosol optical properties and aerosol CCN activity are investigated using datasets on aerosol PNSD measured during several campaigns in the North China Plain. The relationship between σ_{sp} , \AA , κ_c and N_{CCN} is analyzed. It is found that the ratio between N_{CCN} and σ_{sp} , referred to as AR_{sp} , is determined by κ_c and \AA . In light of this, it is possible to calculate N_{CCN} based only on measurements of a three-wavelength humidified nephelometer system which provides information about σ_{sp} , the hygroscopicity parameter κ and \AA . However, κ derived from measurements of a humidified nephelometer system under sub-saturated conditions (termed κ_f) differs from κ under supersaturated conditions, which indicate aerosol CCN activity (termed κ_c). As a result, the conversion from κ_f to κ_c is needed. Based on previous studies of aerosol hygroscopicity and aerosol CCN activity, a simple conversion from κ_f to κ_c with a fixed difference (referred to as $\Delta\kappa$) of 0.2 is proposed. On the basis of this simple conversion, the method of N_{CCN} prediction based only on measurements of a humidified nephelometer system is achieved under conditions without sea salt aerosol, dust aerosol, externally mixed aerosol or fresh aerosol.

This method is validated with measurements of a humidified nephelometer system and a CCN counter in Gucheng in 2016. During the campaign, both N_{CCN} and σ_{sp} vary with the pollution conditions. AR_{sp} is around 5 and changes with \AA and κ_f . Based on this new method, N_{CCN} are calculated to compare with its measured values. The agreement between the calculated N_{CCN} and the measured N_{CCN} is achieved with relative deviations less than 30%. Furthermore, the variation of $\Delta\kappa$ and its influence on N_{CCN} calculation are studied. The difference between κ_f and κ_c was 0.2 ± 0.1 . Sensitivity of calculated N_{CCN} to conversions from κ_f to κ_c is studied by applying different kinds of conversions. Results show that calculated N_{CCN} varies little and is insensitive to the conversions, which confirms the robustness and applicability of this newly proposed method.

This study has connected aerosol optical properties with N_{CCN} and also proposed a novel method to calculate N_{CCN} based only on measurements of a three-wavelength humidi-

fied nephelometer system. Due to the simple operation and stability of the humidified nephelometer system, this method will facilitate the real-time monitoring of N_{CCN} , especially on aircrafts. In addition, measurements of the widely used CCN counter are limited to supersaturations higher than 0.07. In fogs and shallow layer clouds, supersaturations are generally smaller than 0.1% (Ditas et al., 2012; Hammer et al., 2014a, b; Krüger et al., 2014). For studying aerosol–cloud interaction, this method is more applicable due to its applicability for calculating N_{CCN} at lower supersaturations than 1.0%.

Data availability. The corresponding data in Fig. 2 can be accessed through the following link: <https://pan.baidu.com/s/1mjyQ8uk>. The whole dataset can be accessed by request to the corresponding author.

Competing interests. The authors declare that they have no conflict of interest.

Acknowledgements. This work was supported by the National Natural Science Foundation of China (41590872 and 41505107).

Edited by: Pierre Herckes

Reviewed by: two anonymous referees

References

- Andreae, M. O.: Correlation between cloud condensation nuclei concentration and aerosol optical thickness in remote and polluted regions, *Atmos. Chem. Phys.*, 9, 543–556, <https://doi.org/10.5194/acp-9-543-2009>, 2009.
- Andreae, M. O. and Rosenfeld, D.: Aerosol-cloud-precipitation interactions. Part 1. The nature and sources of cloud-active aerosols, *Earth-Sci. Rev.*, 89, 13–41, <https://doi.org/10.1016/j.earscirev.2008.03.001>, 2008.
- Brock, C. A., Wagner, N. L., Anderson, B. E., Attwood, A. R., Beyersdorf, A., Campuzano-Jost, P., Carlton, A. G., Day, D. A., Diskin, G. S., Gordon, T. D., Jimenez, J. L., Lack, D. A., Liao, J., Markovic, M. Z., Middlebrook, A. M., Ng, N. L., Perring, A. E., Richardson, M. S., Schwarz, J. P., Washenfelder, R. A., Welti, A., Xu, L., Ziemba, L. D., and Murphy, D. M.: Aerosol optical properties in the southeastern United States in summer – Part 1: Hygroscopic growth, *Atmos. Chem. Phys.*, 16, 4987–5007, <https://doi.org/10.5194/acp-16-4987-2016>, 2016.
- Chen, J., Zhao, C. S., Ma, N., and Yan, P.: Aerosol hygroscopicity parameter derived from the light scattering enhancement factor measurements in the North China Plain, *Atmos. Chem. Phys.*, 14, 8105–8118, <https://doi.org/10.5194/acp-14-8105-2014>, 2014.
- Cheng, Y. F., Wiedensohler, A., Eichler, H., Su, H., Gnauk, T., Brüeggemann, E., Herrmann, H., Heintzenberg, J., Slanina, J., Tuch, T., Hu, M., and Zhang, Y. H.: Aerosol optical properties and related chemical apportionment at Xinken in

- Pearl River Delta of China, *Atmos. Environ.*, 42, 6351–6372, <https://doi.org/10.1016/j.atmosenv.2008.02.034>, 2008.
- Covert, D. S., Charlson, R., and Ahlquist, N.: A study of the relationship of chemical composition and humidity to light scattering by aerosols, *J. Appl. Meteorol.*, 11, 968–976, 1972.
- Cubison, M. J., Ervens, B., Feingold, G., Docherty, K. S., Ulbrich, I. M., Shields, L., Prather, K., Hering, S., and Jimenez, J. L.: The influence of chemical composition and mixing state of Los Angeles urban aerosol on CCN number and cloud properties, *Atmos. Chem. Phys.*, 8, 5649–5667, <https://doi.org/10.5194/acp-8-5649-2008>, 2008.
- Deng, Z. Z., Zhao, C. S., Ma, N., Liu, P. F., Ran, L., Xu, W. Y., Chen, J., Liang, Z., Liang, S., Huang, M. Y., Ma, X. C., Zhang, Q., Quan, J. N., Yan, P., Henning, S., Mildnerberger, K., Sommerhage, E., Schäfer, M., Stratmann, F., and Wiedensohler, A.: Size-resolved and bulk activation properties of aerosols in the North China Plain, *Atmos. Chem. Phys.*, 11, 3835–3846, <https://doi.org/10.5194/acp-11-3835-2011>, 2011.
- Deng, Z. Z., Zhao, C. S., Ma, N., Ran, L., Zhou, G. Q., Lu, D. R., and Zhou, X. J.: An examination of parameterizations for the CCN number concentration based on in situ measurements of aerosol activation properties in the North China Plain, *Atmos. Chem. Phys.*, 13, 6227–6237, <https://doi.org/10.5194/acp-13-6227-2013>, 2013.
- Ditas, F., Shaw, R. A., Siebert, H., Simmel, M., Wehner, B., and Wiedensohler, A.: Aerosols-cloud microphysics-thermodynamics-turbulence: evaluating supersaturation in a marine stratocumulus cloud, *Atmos. Chem. Phys.*, 12, 2459–2468, <https://doi.org/10.5194/acp-12-2459-2012>, 2012.
- Dusek, U., Frank, G., Hildebrandt, L., Curtius, J., Schneider, J., Walter, S., Chand, D., Drewnick, F., Hings, S., and Jung, D.: Size matters more than chemistry for cloud-nucleating ability of aerosol particles, *Science*, 312, 1375–1378, 2006.
- Ervens, B., Cubison, M., Andrews, E., Feingold, G., Ogren, J. A., Jimenez, J. L., DeCarlo, P., and Nenes, A.: Prediction of cloud condensation nucleus number concentration using measurements of aerosol size distributions and composition and light scattering enhancement due to humidity, *J. Geophys. Res.-Atmos.*, 112, D10S32, <https://doi.org/10.1029/2006jd007426>, 2007.
- Ervens, B., Cubison, M. J., Andrews, E., Feingold, G., Ogren, J. A., Jimenez, J. L., Quinn, P. K., Bates, T. S., Wang, J., Zhang, Q., Coe, H., Flynn, M., and Allan, J. D.: CCN predictions using simplified assumptions of organic aerosol composition and mixing state: a synthesis from six different locations, *Atmos. Chem. Phys.*, 10, 4795–4807, <https://doi.org/10.5194/acp-10-4795-2010>, 2010.
- Ferrero, L., Castelli, M., Ferrini, B. S., Moscatelli, M., Perrone, M. G., Sangiorgi, G., D'Angelo, L., Rovelli, G., Moroni, B., Scardazza, F., Mocnik, G., Bolzacchini, E., Petitta, M., and Cappelletti, D.: Impact of black carbon aerosol over Italian basin valleys: high-resolution measurements along vertical profiles, radiative forcing and heating rate, *Atmos. Chem. Phys.*, 14, 9641–9664, <https://doi.org/10.5194/acp-14-9641-2014>, 2014.
- Gasso, S. and Hegg, D. A.: On the retrieval of columnar aerosol mass and CCN concentration by MODIS, *J. Geophys. Res.-Atmos.*, 108, 4010, <https://doi.org/10.1029/2002jd002382>, 2003.
- Ghan, S. J. and Collins, D. R.: Use of in situ data to test a Raman lidar-based cloud condensation nuclei remote sensing method, *J. Atmos. Ocean. Tech.*, 21, 387–394, [https://doi.org/10.1175/1520-0426\(2004\)021<0387:uoisd>2.0.co;2](https://doi.org/10.1175/1520-0426(2004)021<0387:uoisd>2.0.co;2), 2004.
- Ghan, S. J., Rissman, T. A., Elleman, R., Ferrare, R. A., Turner, D., Flynn, C., Wang, J., Ogren, J., Hudson, J., Jonsson, H. H., VanReken, T., Flagan, R. C., and Seinfeld, J. H.: Use of in situ cloud condensation nuclei, extinction, and aerosol size distribution measurements to test a method for retrieving cloud condensation nuclei profiles from surface measurements, *J. Geophys. Res.-Atmos.*, 111, D05s10, <https://doi.org/10.1029/2004jd005752>, 2006.
- Good, N., Topping, D. O., Allan, J. D., Flynn, M., Fuentes, E., Irwin, M., Williams, P. I., Coe, H., and McFiggans, G.: Consistency between parameterisations of aerosol hygroscopicity and CCN activity during the RHAMBLe discovery cruise, *Atmos. Chem. Phys.*, 10, 3189–3203, <https://doi.org/10.5194/acp-10-3189-2010>, 2010.
- Gunthe, S. S., King, S. M., Rose, D., Chen, Q., Roldin, P., Farmer, D. K., Jimenez, J. L., Artaxo, P., Andreae, M. O., Martin, S. T., and Pöschl, U.: Cloud condensation nuclei in pristine tropical rainforest air of Amazonia: size-resolved measurements and modeling of atmospheric aerosol composition and CCN activity, *Atmos. Chem. Phys.*, 9, 7551–7575, <https://doi.org/10.5194/acp-9-7551-2009>, 2009.
- Hudson, J. G.: An instantaneous ccn spectrometer, *J. Atmos. Ocean. Tech.*, 6, 1055–1065, [https://doi.org/10.1175/1520-0426\(1989\)006<1055:aics>2.0.co;2](https://doi.org/10.1175/1520-0426(1989)006<1055:aics>2.0.co;2), 1989.
- Hammer, E., Bukowiecki, N., Gysel, M., Jurányi, Z., Hoyle, C. R., Vogt, R., Baltensperger, U., and Weingartner, E.: Investigation of the effective peak supersaturation for liquid-phase clouds at the high-alpine site Jungfrauoch, Switzerland (3580 m a.s.l.), *Atmos. Chem. Phys.*, 14, 1123–1139, <https://doi.org/10.5194/acp-14-1123-2014>, 2014a.
- Hammer, E., Gysel, M., Roberts, G. C., Elias, T., Hofer, J., Hoyle, C. R., Bukowiecki, N., Dupont, J.-C., Burnet, F., Baltensperger, U., and Weingartner, E.: Size-dependent particle activation properties in fog during the ParisFog 2012/13 field campaign, *Atmos. Chem. Phys.*, 14, 10517–10533, <https://doi.org/10.5194/acp-14-10517-2014>, 2014b.
- Irwin, M., Good, N., Crosier, J., Choularton, T. W., and McFiggans, G.: Reconciliation of measurements of hygroscopic growth and critical supersaturation of aerosol particles in central Germany, *Atmos. Chem. Phys.*, 10, 11737–11752, <https://doi.org/10.5194/acp-10-11737-2010>, 2010.
- Jefferson, A.: Empirical estimates of CCN from aerosol optical properties at four remote sites, *Atmos. Chem. Phys.*, 10, 6855–6861, <https://doi.org/10.5194/acp-10-6855-2010>, 2010.
- Kapustin, V. N., Clarke, A. D., Shinzuka, Y., Howell, S., Brekhovskikh, V., Nakajima, T., and Higurashi, A.: On the determination of a cloud condensation nuclei from satellite: Challenges and possibilities, *J. Geophys. Res.-Atmos.*, 111, D04202, <https://doi.org/10.1029/2004jd005527>, 2006.
- Köhler, H.: The nucleus in and the growth of hygroscopic droplets, *T. Faraday Soc.*, 32, 1152–1161, 1936.
- Kreidenweis, S. M. and Asa-Awuku, A.: 5.13 – Aerosol Hygroscopicity: Particle Water Content and Its Role in Atmospheric Processes A2 – Holland, Heinrich D, in: *Treatise on Geochemistry*, 2nd Edn., edited by: Turekian, K. K., Elsevier, Oxford, 331–361, 2014.

- Krüger, M. L., Mertes, S., Klimach, T., Cheng, Y. F., Su, H., Schneider, J., Andreae, M. O., Pöschl, U., and Rose, D.: Assessment of cloud supersaturation by size-resolved aerosol particle and cloud condensation nuclei (CCN) measurements, *Atmos. Meas. Tech.*, 7, 2615–2629, <https://doi.org/10.5194/amt-7-2615-2014>, 2014.
- Kuang, Y., Zhao, C. S., Ma, N., Liu, H. J., Bian, Y. X., Tao, J. C., and Hu, M.: Deliquescent phenomena of ambient aerosols on the North China Plain, *Geophys. Res. Lett.*, 43, 8744–8750, <https://doi.org/10.1002/2016gl070273>, 2016.
- Kuang, Y., Zhao, C., Tao, J., Bian, Y., Ma, N., and Zhao, G.: A novel method for deriving the aerosol hygroscopicity parameter based only on measurements from a humidified nephelometer system, *Atmos. Chem. Phys.*, 17, 6651–6662, <https://doi.org/10.5194/acp-17-6651-2017>, 2017a.
- Kuang, Y., Zhao, C., Tao, J., Bian, Y., Ma, N., and Zhao, G.: A novel method for deriving the aerosol hygroscopicity parameter based only on measurements from a humidified nephelometer system, *Atmos. Chem. Phys.*, 17, 6651–6662, <https://doi.org/10.5194/acp-17-6651-2017>, 2017b.
- Lance, S., Nenes, A., Medina, J., and Smith, J.: Mapping the operation of the DMT continuous flow CCN counter, *Aerosol Sci. Tech.*, 40, 242–254, 2006.
- Latham, T. L. and Nenes, A.: Water Vapor Depletion in the DMT Continuous-Flow CCN Chamber: Effects on Supersaturation and Droplet Growth, *Aerosol Sci. Tech.*, 45, 604–615, <https://doi.org/10.1080/02786826.2010.551146>, 2011.
- Liu, H. J., Zhao, C. S., Nekat, B., Ma, N., Wiedensohler, A., van Pinxteren, D., Spindler, G., Müller, K., and Herrmann, H.: Aerosol hygroscopicity derived from size-segregated chemical composition and its parameterization in the North China Plain, *Atmos. Chem. Phys.*, 14, 2525–2539, <https://doi.org/10.5194/acp-14-2525-2014>, 2014.
- Liu, J. and Li, Z.: Estimation of cloud condensation nuclei concentration from aerosol optical quantities: influential factors and uncertainties, *Atmos. Chem. Phys.*, 14, 471–483, <https://doi.org/10.5194/acp-14-471-2014>, 2014.
- Ma, N., Zhao, C. S., Nowak, A., Müller, T., Pfeifer, S., Cheng, Y. F., Deng, Z. Z., Liu, P. F., Xu, W. Y., Ran, L., Yan, P., Göbel, T., Hallbauer, E., Mildnerberger, K., Henning, S., Yu, J., Chen, L. L., Zhou, X. J., Stratmann, F., and Wiedensohler, A.: Aerosol optical properties in the North China Plain during HaChi campaign: an in-situ optical closure study, *Atmos. Chem. Phys.*, 11, 5959–5973, <https://doi.org/10.5194/acp-11-5959-2011>, 2011.
- Ma, N., Zhao, C., Tao, J., Wu, Z., Kecorius, S., Wang, Z., Groß, J., Liu, H., Bian, Y., Kuang, Y., Teich, M., Spindler, G., Müller, K., van Pinxteren, D., Herrmann, H., Hu, M., and Wiedensohler, A.: Variation of CCN activity during new particle formation events in the North China Plain, *Atmos. Chem. Phys.*, 16, 8593–8607, <https://doi.org/10.5194/acp-16-8593-2016>, 2016.
- McMeeking, G. R., Morgan, W. T., Flynn, M., Highwood, E. J., Turnbull, K., Haywood, J., and Coe, H.: Black carbon aerosol mixing state, organic aerosols and aerosol optical properties over the United Kingdom, *Atmos. Chem. Phys.*, 11, 9037–9052, <https://doi.org/10.5194/acp-11-9037-2011>, 2011.
- Moteki, N. and Kondo, Y.: Effects of Mixing State on Black Carbon Measurements by Laser-Induced Incandescence, *Aerosol Sci. Tech.*, 41, 398–417, <https://doi.org/10.1080/02786820701199728>, 2007.
- Nenes, A., Chuang, P. Y., Flagan, R. C., and Seinfeld, J. H.: A theoretical analysis of cloud condensation nucleus (CCN) instruments, *J. Geophys. Res.-Atmos.*, 106, 3449–3474, <https://doi.org/10.1029/2000jd900614>, 2001.
- Petters, M. D. and Kreidenweis, S. M.: A single parameter representation of hygroscopic growth and cloud condensation nucleus activity, *Atmos. Chem. Phys.*, 7, 1961–1971, <https://doi.org/10.5194/acp-7-1961-2007>, 2007.
- Roberts, G. and Nenes, A.: A continuous-flow streamwise thermal-gradient CCN chamber for atmospheric measurements, *Aerosol Sci. Tech.*, 39, 206–221, 2005.
- Rose, D., Gunthe, S. S., Mikhailov, E., Frank, G. P., Dusek, U., Andreae, M. O., and Pöschl, U.: Calibration and measurement uncertainties of a continuous-flow cloud condensation nuclei counter (DMT-CCNC): CCN activation of ammonium sulfate and sodium chloride aerosol particles in theory and experiment, *Atmos. Chem. Phys.*, 8, 1153–1179, <https://doi.org/10.5194/acp-8-1153-2008>, 2008.
- Rose, D., Nowak, A., Achtert, P., Wiedensohler, A., Hu, M., Shao, M., Zhang, Y., Andreae, M. O., and Pöschl, U.: Cloud condensation nuclei in polluted air and biomass burning smoke near the mega-city Guangzhou, China – Part 1: Size-resolved measurements and implications for the modeling of aerosol particle hygroscopicity and CCN activity, *Atmos. Chem. Phys.*, 10, 3365–3383, <https://doi.org/10.5194/acp-10-3365-2010>, 2010.
- Renbaum-Wolff, L., Song, M., Marcolli, C., Zhang, Y., Liu, P. F., Grayson, J. W., Geiger, F. M., Martin, S. T., and Bertram, A. K.: Observations and implications of liquid-liquid phase separation at high relative humidities in secondary organic material produced by α -pinene ozonolysis without inorganic salts, *Atmos. Chem. Phys.*, 16, 7969–7979, <https://doi.org/10.5194/acp-16-7969-2016>, 2016.
- Shinozuka, Y., Clarke, A. D., Nenes, A., Jefferson, A., Wood, R., McNaughton, C. S., Ström, J., Tunved, P., Redemann, J., Thornhill, K. L., Moore, R. H., Latham, T. L., Lin, J. J., and Yoon, Y. J.: The relationship between cloud condensation nuclei (CCN) concentration and light extinction of dried particles: indications of underlying aerosol processes and implications for satellite-based CCN estimates, *Atmos. Chem. Phys.*, 15, 7585–7604, <https://doi.org/10.5194/acp-15-7585-2015>, 2015.
- Titos, G., Cazorla, A., Zieger, P., Andrews, E., Lyamani, H., Granados-Muñoz, M. J., Olmo, F. J., and Alados-Arboledas, L.: Effect of hygroscopic growth on the aerosol light-scattering coefficient: A review of measurements, techniques and error sources, *Atmos. Environ.*, 141, 494–507, <https://doi.org/10.1016/j.atmosenv.2016.07.021>, 2016.
- Wex, H., McFiggans, G., Henning, S., and Stratmann, F.: Influence of the external mixing state of atmospheric aerosol on derived CCN number concentrations, *Geophys. Res. Lett.*, 37, L10805, <https://doi.org/10.1029/2010gl043337>, 2010.

- Whitehead, J. D., Irwin, M., Allan, J. D., Good, N., and McFiggans, G.: A meta-analysis of particle water uptake reconciliation studies, *Atmos. Chem. Phys.*, 14, 11833–11841, <https://doi.org/10.5194/acp-14-11833-2014>, 2014.
- Wu, Z. J., Poulain, L., Henning, S., Dieckmann, K., Birmili, W., Merkel, M., van Pinxteren, D., Spindler, G., Müller, K., Stratmann, F., Herrmann, H., and Wiedensohler, A.: Relating particle hygroscopicity and CCN activity to chemical composition during the HCCT-2010 field campaign, *Atmos. Chem. Phys.*, 13, 7983–7996, <https://doi.org/10.5194/acp-13-7983-2013>, 2013.